

**Microstructural Study on Dynamic Recrystallization
and Texture Formation in Pure Nickel**

Makoto Hasegawa and Hiroshi Fukutomi

Reprinted from

MATERIALS TRANSACTIONS, VOL. 43 NO. 5, MAY, 2002

THE JAPAN INSTITUTE OF METALS

Aoba Aramaki, Aoba-ku, Sendai 980-0845, Japan

Microstructural Study on Dynamic Recrystallization and Texture Formation in Pure Nickel *1

Makoto Hasegawa *2 and Hiroshi Fukutomi

Division of Materials Science and Engineering, Graduate School of Yokohama National University, Yokohama 240-8501, Japan

Dynamic recrystallization and resultant texture formation were studied by high temperature compressive deformation of pure nickel. Microstructural observation and orientation measurement revealed that grain boundaries become wavy during deformation and the deformation inhomogeneity is enhanced in the vicinity of wavy boundaries where new grains nucleate with random orientation. These grains grow up during deformation and after reaching a certain size new grains are formed again near the grain boundaries of grown up grains. This process occurs repeatedly during dynamic recrystallization. Concerning texture, randomly oriented new grains receive compressive deformation and change their orientation toward the stable orientation for compression (011). However, further grain nucleation occurs in random orientation before they reach (011); grains whose orientations are close to (011) disappear.

(Received January 7, 2002; Accepted March 11, 2002)

Keywords: pure nickel, dynamic recrystallization, nucleation, texture, electron backscattering pattern, grain boundary curvature, inhomogeneous deformation

1. Introduction

Some of mechanical and structural characteristics of dynamic recrystallization (hereafter abbreviated as DRX) have been made clear in some metals and alloys on the basis of the analysis of stress-strain curves and microstructural observation.¹⁾ It is considered that DRX proceeds through the following processes (1) to (4):²⁾ (1) new grain formation in the vicinity of initial grain boundaries, (2) continuous occurrence of further grain formation in the front regions of the previously recrystallized areas, (3) total replacement of initial grains by the newly formed grains and (4) further DRX in the fully DRXed matrices. However, there still remain many indistinct points on the details of these processes.

It has been found that the grain boundary becomes wavy prior to the nucleation of new grains in its vicinity,³⁾ and this is considered to be important for the formation of new grains although no special attention has been seldom paid to the phenomenon. Only a few works^{4,5)} have been done in which the importance of grain boundaries is taken into consideration.

The present authors examined microstructure and texture formed during uniaxial compression of pure nickel polycrystals over wide ranges of temperatures (873 K to 1573 K) and strain rates ($2.5 \times 10^{-5} \text{ s}^{-1}$ to $1.0 \times 10^{-3} \text{ s}^{-1}$).⁶⁾ At deformation conditions of low temperature and high strain rate, DRX was considered to occur by the so-called nucleation and growth mechanism and new grains did not have any preferred orientations. In the previous work, however, the reason why new grains are formed in random orientation near the grain boundary was not made clear. In the present work, changes in the microstructure and crystal orientation with the progress of DRX were examined for understanding the detailed processes of DRX and resultant texture formation.

2. Experimental Procedure

2.1 Material and compression test

Pure nickel of 99.9 mass% purity is used for the test. Cylindrical specimens with a diameter of 8 mm and a height of 12 mm were machined from a rod annealed at 1073 K for 3.6 ks. The average grain size after the annealing was 63 μm .

Uniaxial compression tests were conducted in vacuum at temperatures of 873 K and 905 K and true strain rate of $1.0 \times 10^{-4} \text{ s}^{-1}$ and $1.0 \times 10^{-3} \text{ s}^{-1}$. For comparison, some specimens were deformed also at room temperature. Specimens were held for 15 min at the testing temperatures before the start of test. Immediately after straining up to a predetermined strain, specimens were blown with helium gas for freezing the microstructure in the midst of deformation; the specimen was cooled down from 905 K to 573 K within 11 sec and the static recrystallization during cooling down could be successfully prevented.

2.2 Structural observation and crystal orientation measurement

After the tests, planes mid-plane sections were obtained by machining, for the microstructure observations by optical microscopy and SEM, and crystal orientation measurements by EBSP technique.

Local crystal orientations of very small regions were measured by EBSP technique. Measurements were done at intervals of 1 μm or 2 μm , and the minimum rotation angle θ between neighboring points was calculated. When θ between 5° and 12°, it was judged that a low angle boundary exists between the two point in the identical crystal grain. When θ is above 12°, the boundary was defined as a high angle grain boundary. Figures were drawn from the information on the position and shape of grains both of which were determined by the orientation measurement. These figures are called "grain structure micrographs" in the present paper. The upper limit of θ for low angle boundaries (12 degrees) was chosen since the grain boundary micrograph well coincides

*1 This Paper was Originally Published in J. Japan Inst. Metals 65 (2001) 1014-1022.

*2 Graduate Student, Yokohama National University.

with the micrograph obtained by OM and SEM at this value of θ .

To determine the orientation distribution in the early stage of DRX, crystal orientations were measured by shifting the point of measurement along and normal to initial grain boundaries. Further, the orientation was measured in many grains of the fully DRXed specimen, and the dependence of texture on the grain size was studied by drawing inverse pole figure for each of 5 classes of grain size (3–5, 5–10, 10–20, 20–50 and 50–100 μm)

2.3 Degree of grain boundary curvature

It has been known³⁾ that, prior to the start of DRX, grain boundaries become wavy during deformation. To know the effect of such undulation of grain boundaries on DRX, the orientation distribution was examined as a function of a degree of grain boundary curvature that was defined as h/w where h and w are a height and a width of curvature given in Fig. 1, respectively. A preliminary experiment showed that, after deformation up to -0.85 at 873 K and a true strain rate of $1.0 \times 10^{-3} \text{ s}^{-1}$, a width of the curvature w was in a range of 1–18 μm and about 97% of w was smaller than 10 μm . The distribution of h/w is given in Fig. 2. A fraction of h/w takes a maximum in a range between 0.2–0.4 and amounts to about 47%. In the present work, therefore, the orientation distribution near grain boundaries was examined for each of three ranges of h/w , that is $h/w < 0.2$, $0.2 \leq h/w < 0.4$ and $0.4 \leq h/w$.

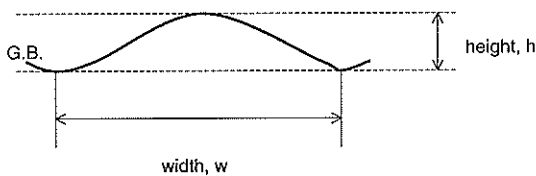


Fig. 1 Definition of the degree of grain boundary curvature h/w ; h and w are height and width of curvature, respectively.

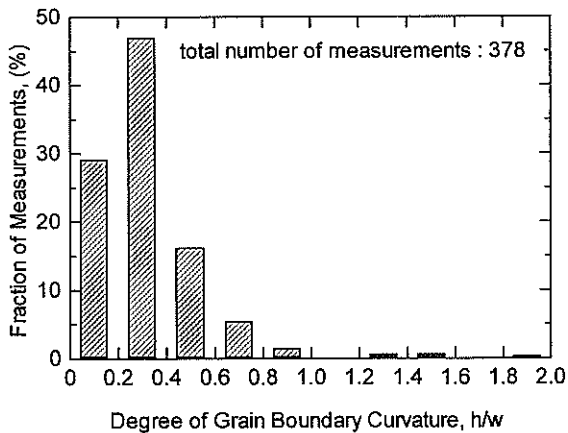


Fig. 2 Histogram showing the distribution of the degree of grain boundary curvature after compression test of pure nickel at 873 K with a true strain rate of $1.0 \times 10^{-3} \text{ s}^{-1}$ up to a true strain of -0.85 . About 97% of w was less than 10 μm .

3. Experimental Results

3.1 Stress-strain behavior

Figure 3 shows true stress-true strain curves at various temperatures. As seen in the figure, severe work-hardening occurs in the room temperature deformation at a true strain rate of $1.0 \times 10^{-3} \text{ s}^{-1}$. At high temperatures, on the other hand, the curves are the so-called work-softening type in nature regardless of the strain rate; the flow stress takes a maximum at an initial stage of deformation, and then decreases with the further straining. The softening has been found to be due to DRX.⁶⁾

3.2 Change in microstructure during deformation

Photomicrographs taken before and after the deformation are given in Figs. 4(a) and (b)–(d), respectively. Before deformation, microstructure consists of equiaxed grains (average size: 63 μm) with smooth boundaries (Fig. 4(a)). Annealing twins are also seen. After room temperature deformation up to a true strain of -0.94 during which no DRX occurred, grain boundaries are still smooth, though they are gently bowed (Fig. 4(b)). Figure 4(c) shows microstructure at an early stage of DRX after deformation up to a strain of -0.85 at 873 K and a strain rate of $1.0 \times 10^{-3} \text{ s}^{-1}$. It is seen that, during deformation, grain boundaries became wavy. This may be due to an energy balance between the grain boundary and the subboundaries that were formed in the grain interior.⁷⁾ Further, it is noteworthy that very small grains were newly formed near grain boundaries. After deformation up to a larger strain of -1.7 at a higher temperature of 905 K and a lower strain rate of $1.0 \times 10^{-4} \text{ s}^{-1}$, the initial, statically recrystallized structure was fully encroached by the DRXed structure consisting of smaller grains (average size: 17 μm) with severely waved grain boundaries (Fig. 4(d)).

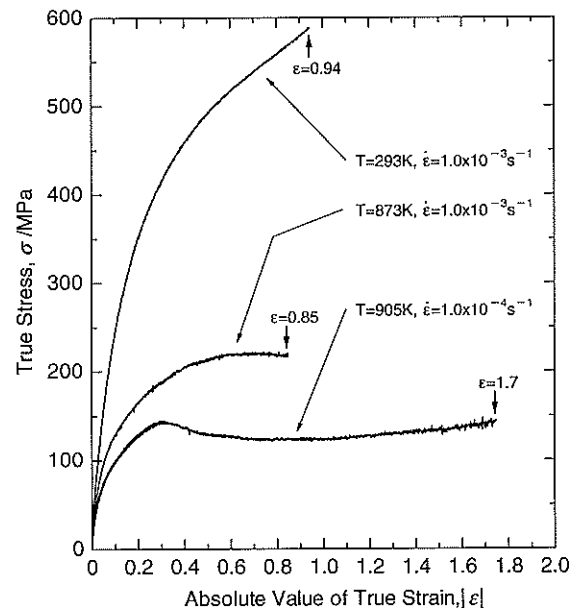


Fig. 3 True stress-true strain curves of pure nickel obtained by compression tests at various temperatures and true strain rates.

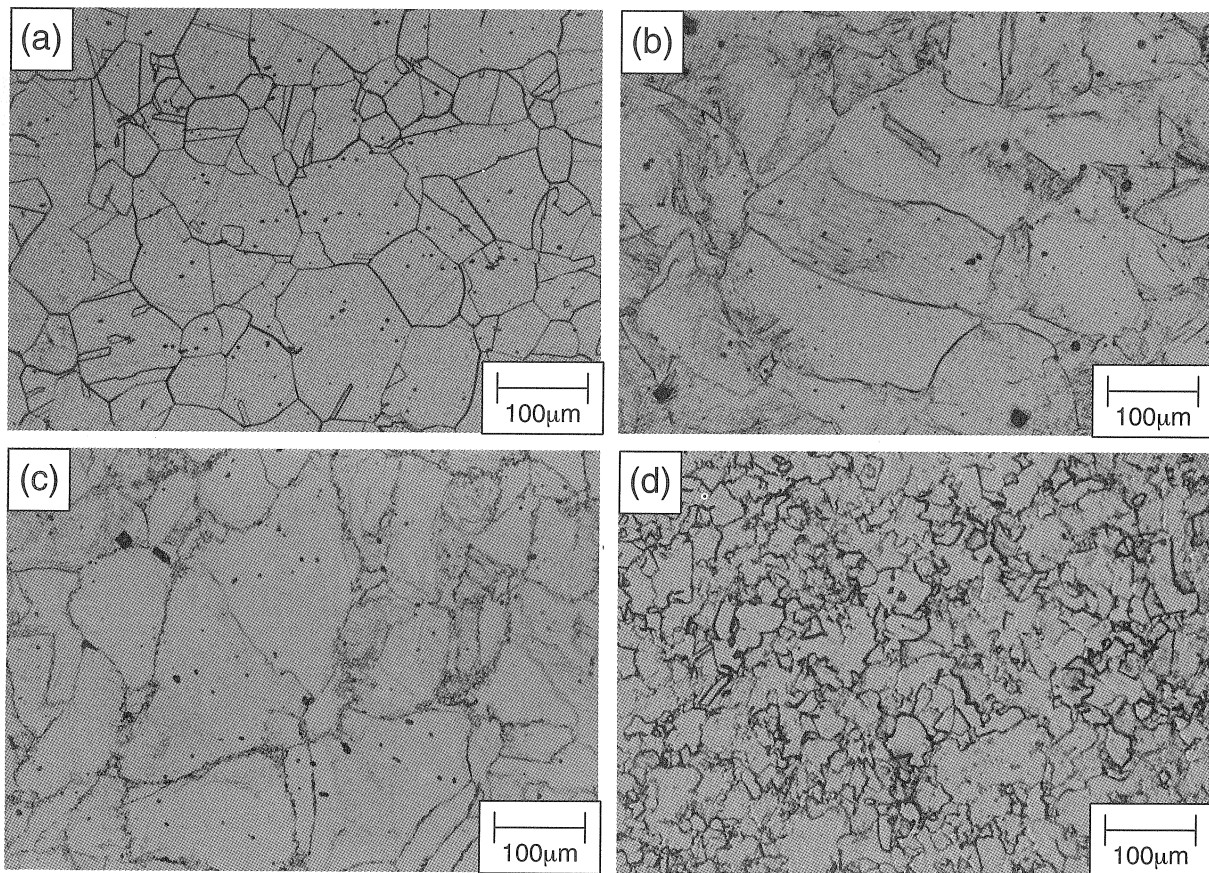


Fig. 4 Optical micrographs of pure nickel before compression (a) and after compression (b)–(d). (b) Temperature $T = 293$ K, true strain rate $\dot{\epsilon} = 1.0 \times 10^{-3} \text{ s}^{-1}$, true strain $\epsilon = -0.94$; (c) $T = 873$ K, $\dot{\epsilon} = 1.0 \times 10^{-3} \text{ s}^{-1}$, $\epsilon = -0.85$ and (d) $T = 905$ K, $\dot{\epsilon} = 1.0 \times 10^{-4} \text{ s}^{-1}$, $\epsilon = -1.7$.

3.3 Crystal orientation after room temperature deformation

Distribution of crystal orientation along grain boundaries was measured for 23 grain boundaries after the deformation at room temperature up to a strain of -0.94 in which no DRX occurred. An example of the results is given in Fig. 5. Grain boundaries are rather smooth as seen in Figs. 5(a) and (b), which are SEM micrograph and grain structure micrograph of the same area, respectively. Crystal orientation was measured at points 1–16 in Fig. 5(b), and the misorientation θ and the rotation axis between neighboring points (interval: $3\text{--}5 \mu\text{m}$) are shown in Figs. 5(c) and (d). It is seen that the misorientation θ is about 5° at most and the rotation axis distributes at random. A fact that the value of θ is as small as 5° indicates no formation of new grains even in the vicinity of grain boundaries. In addition, the compression axis became approximately parallel to the orientation of (011) in the central area of almost all grains.

3.4 Crystal orientation after high temperature deformation

3.4.1 Orientation distribution at the early stage of dynamic recrystallization

Crystal orientation was measured in a specimen deformed up to a strain of -0.85 at 873 K and a strain rate of $1.0 \times 10^{-3} \text{ s}^{-1}$ in which DRX occurred only in the vicinity of grain boundaries as seen in Fig. 4(c).

Same kinds of examination as in Fig. 5 were made for 21

grain boundaries, and the typical result is given in Fig. 6. In contrast to room temperature deformation, grain boundaries became wavy during high temperature deformation (Figs. 6(a) and (b)). Crystal orientation was measured at points 1–26 in Fig. 6(b), and the misorientation θ and the rotation axis between neighboring points (interval: $3\text{--}5 \mu\text{m}$) are shown in Figs. 6(c) and (d), respectively. The values of θ are generally larger than those after room temperature deformation, and its maximum amounts to 25° (Fig. 6(c)), indicating the formation of new grains near the grain boundary. As in the high temperature deformation, however, the rotation axis distributes at random (Fig. 6(d)). Further, the compression axis was around the orientation of (011) in the central area of most grains, as in room temperature deformation.

As mentioned in the introduction, the authors considered the change of grain boundary shape during deformation; grain boundaries are wavy through out DRX. The distribution of misorientation θ between neighboring points (interval: $3\text{--}5 \mu\text{m}$) along grain boundaries is depicted in Fig. 7 for different ranges of the grain boundary curvature h/w . Both average and maximum (indicated by an arrow in each figure) values of θ were larger for the case of larger value of h/w .⁸⁾ Further, the fraction of misorientation for $12^\circ \leq \theta$ increased with increasing value of h/w ; 3.7%, 15.0% and 22.6% for $h/w < 0.2$, $0.2 \leq h/w < 0.4$ and $0.4 \leq h/w$, respectively. These facts indicate that in the grain boundary curvature has a strong effect on the degree of the orientation distribution along the grain boundary.

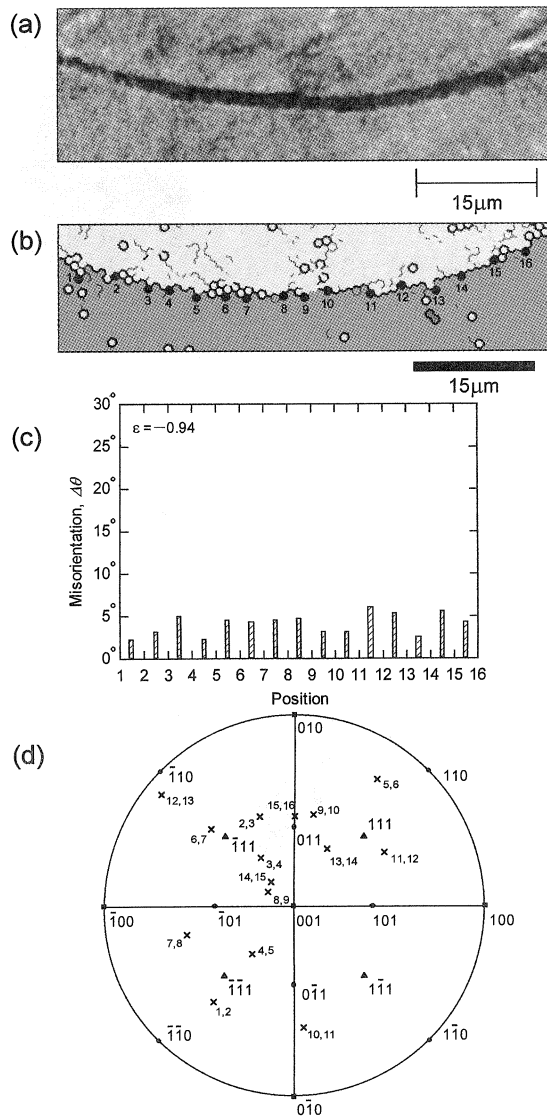


Fig. 5 SEM micrograph of a grain boundary (a) and the same boundary constructed by EBSP (b) in a specimen deformed at room temperature ($T = 293 \text{ K}$, $\dot{\epsilon} = 1.0 \times 10^{-3} \text{ s}^{-1}$, $\epsilon = -0.94$). Positions of orientation measurement are shown in (b). Misorientation and rotation axis between neighboring positions along the boundary are given in (c) and (d), respectively.

To know the extent of grain boundary effect on the orientation distribution, crystal orientation was measured by shifting the point of measurement from the grain boundary to the grain center in 20 grains. An example of the results is given in Fig. 8 for 5 grains. The misorientation θ between neighboring points (interval: 3–5 μm) generally takes a maximum near the grain boundary and decreases with a distance from the grain boundary. At this stage of DRX, the effect of grain boundaries on the misorientation extends about 15 μm from the grain boundaries.

3.4.2 Crystal orientation of new grains formed at the beginning of dynamic recrystallization

Immediately after the occurrence of DRX, crystal orientation of newly formed grains in the vicinity of initial grain boundaries was measured, and its distribution after deformation at 873 K and 905 K is shown in Figs. 9(a) and (b), respectively, in a form of inverse pole figure. The maximum of pole density (P_{MAX}) and its position (α , β) are given below each

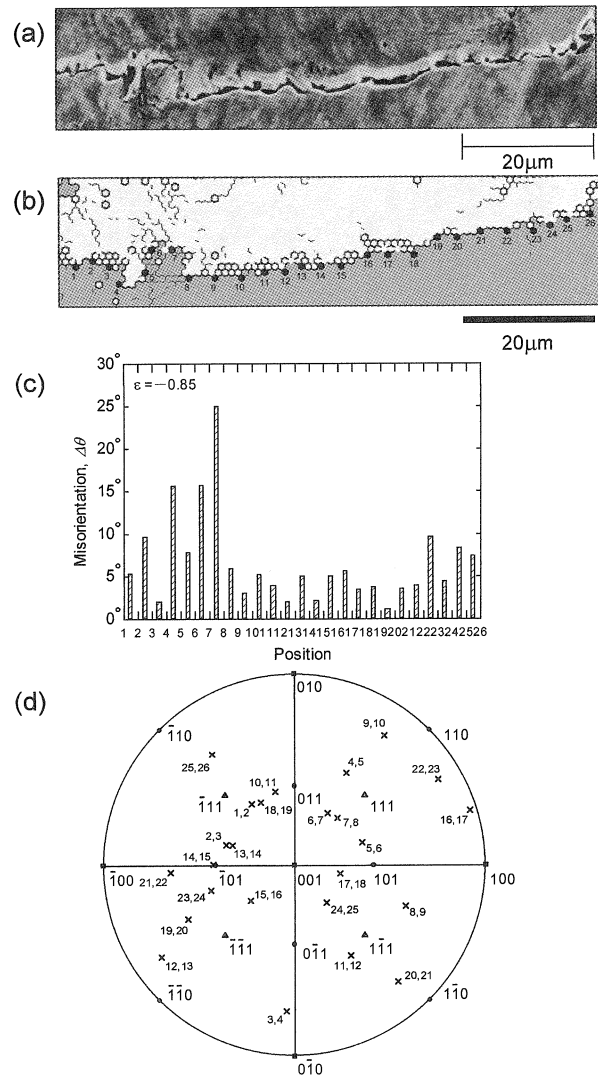


Fig. 6 The figures that are same as those in Fig. 5, for a specimen deformed at high temperature ($T = 873 \text{ K}$, $\dot{\epsilon} = 1.0 \times 10^{-3} \text{ s}^{-1}$, $\epsilon = -0.85$).

figure. The definition of angles, α and β , is given in Fig. 9(c).

The position of maximum pole density seems to be in the orientation of 10–15 degrees away from (011) to (001). However, the value of P_{MAX} is only 1.5–1.8 times of the level for the random orientation distribution, so it can be said that the new grains are formed at almost random orientation.

3.4.3 Dependence of crystal orientation on the grain size in the dynamically recrystallized microstructure

Figure 10 is a grain boundary micrograph after the deformation up to a large strain of -1.7 at 905 K and a strain rate of $1.0 \times 10^{-4} \text{ s}^{-1}$ during which the whole area of the specimen has been recrystallized dynamically. In the figure, thin lines and thick lines represent low angle grain boundaries ($\theta < 12^\circ$) and high angle grain boundaries ($12^\circ \leq \theta$), respectively. The size of dynamically recrystallized grains distributes from a few μm to more than 50 μm. Many of small grains tend to exist together in a group and large grains frequently contain low angle boundaries in their interior. The grain size d was classified into five ranges and each range is represented by the symbols A–E; A: 3–5 μm, B: 5–10 μm, C: 10–20 μm, D: 20–50 μm and E: 50–100 μm.

Figure 11 shows inverse pole figures for each range of the

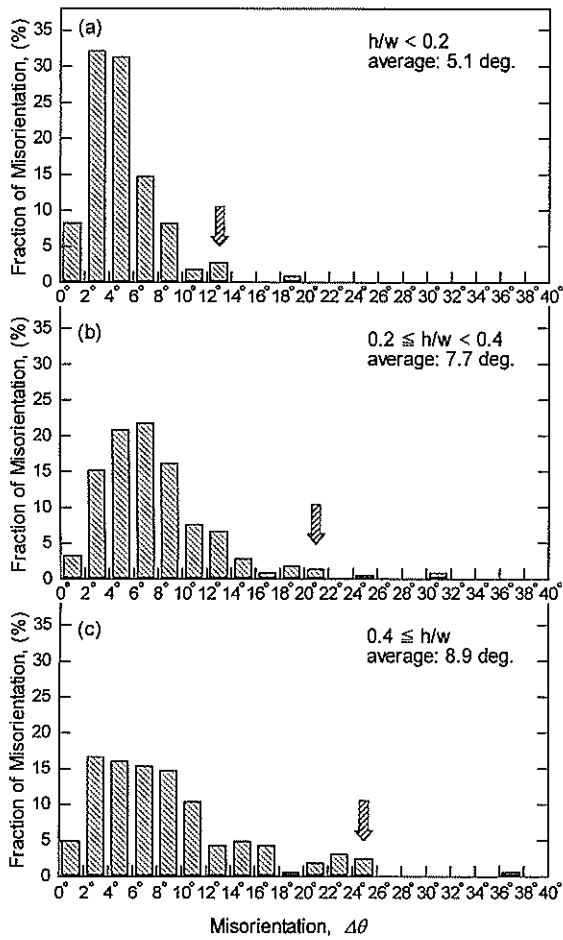


Fig. 7 Histogram showing the distribution of misorientation between neighboring points (in an interval of 3 to 5 μm) along grain boundaries in the specimen deformed at high temperature ($T = 873 \text{ K}$, $\dot{\epsilon} = 1.0 \times 10^{-3} \text{ s}^{-1}$, $\epsilon = -0.85$). Arrows show the maximum value at the continuous distribution from low misorientation angles.

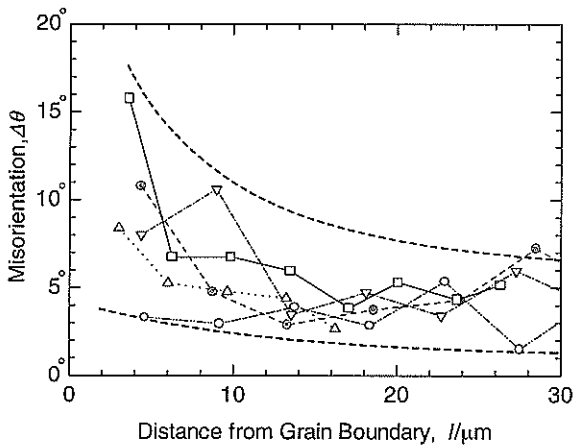


Fig. 8 Misorientation between neighboring positions as a function of distance from grain boundaries toward the center of grains in the specimen deformed at high temperature ($T = 873 \text{ K}$, $\dot{\epsilon} = 1.0 \times 10^{-3} \text{ s}^{-1}$, $\epsilon = -0.85$). Each symbol corresponds to the different grains in which measurement was done.

grain size. Here, the average pole density is used as units. For small grain sizes of the ranges A and B, the main component of the texture is (011) that is the stable orientation for compression. For large grain sizes such as ranges D and E, on the other hand, the position of maximum pole density is in the orientation of 12 degrees away from (011) to (001).

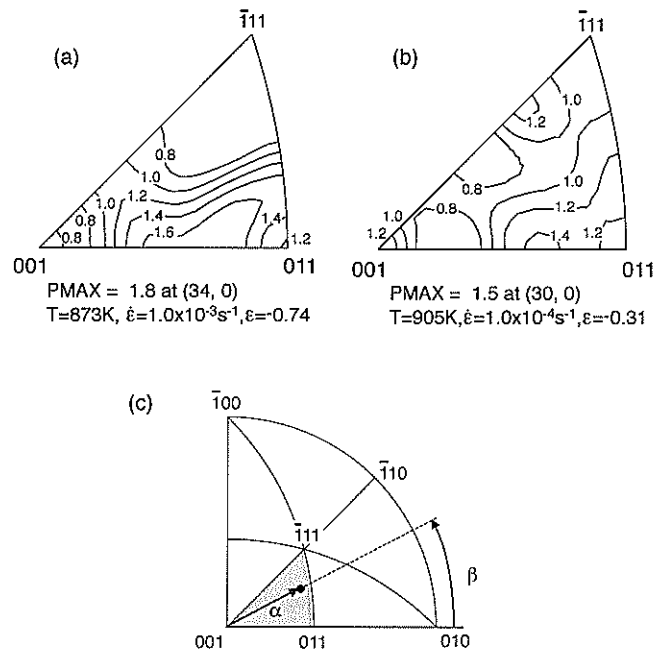


Fig. 9 Inverse pole figures of new grains showing the distribution of pole densities of the compression plane. The average density is used as units. New grains are selected in the specimens compressed at (a) temperature $T = 873 \text{ K}$, true strain rate $\dot{\epsilon} = 1.0 \times 10^{-3} \text{ s}^{-1}$, true strain $\epsilon = -0.74$ and (b) $T = 905 \text{ K}$, $\dot{\epsilon} = 1.0 \times 10^{-4} \text{ s}^{-1}$, $\epsilon = -0.31$. The position of maximum pole density (α , β) is given below the figures. Definitions of the angles, α and β , are shown in (c).

For the intermediate grain size, namely the range C, it is in the middle of the above two orientations on the (001)–(011) line. Tsuji *et al.*⁹ have also found in an Fe-35%Ni alloy that, in the dynamically recrystallized microstructure, the crystal orientation is closer to (011) in smaller grains. The fact that smaller grains have an orientation closer to (011) indicates that smaller grains have been subjected to the larger deformation.

4. Discussion

4.1 Nucleation site and orientation of new grains in dynamic recrystallization

Formation of new grains in the so-called static recrystallization is known to occur preferentially in a region of inhomogeneous deformation such as a shear band, transition band or the area close to grain boundaries. Two prerequisites are generally considered to be necessary for the new grain formation:¹⁰ critical size of nucleus and critical misorientation between nucleus and its surrounding area. As in static recrystallization, the vicinity of initial grain boundary is a preferred nucleation site of new grains also in DRX (see Fig. 4(c)), suggesting that grain boundary takes an important role in DRX. However, only a few works have been reported that pay attention to the importance of grain boundary for discussing the formation process of new grains during DRX.

4.2 Local lattice rotation prior to the formation of new grains in dynamic recrystallization

In the present deformation conditions, the texture is not so sharp in comparison with the results in γ -TiAl; the value of PMAX was only about 3.⁶ In contrast to the deformation

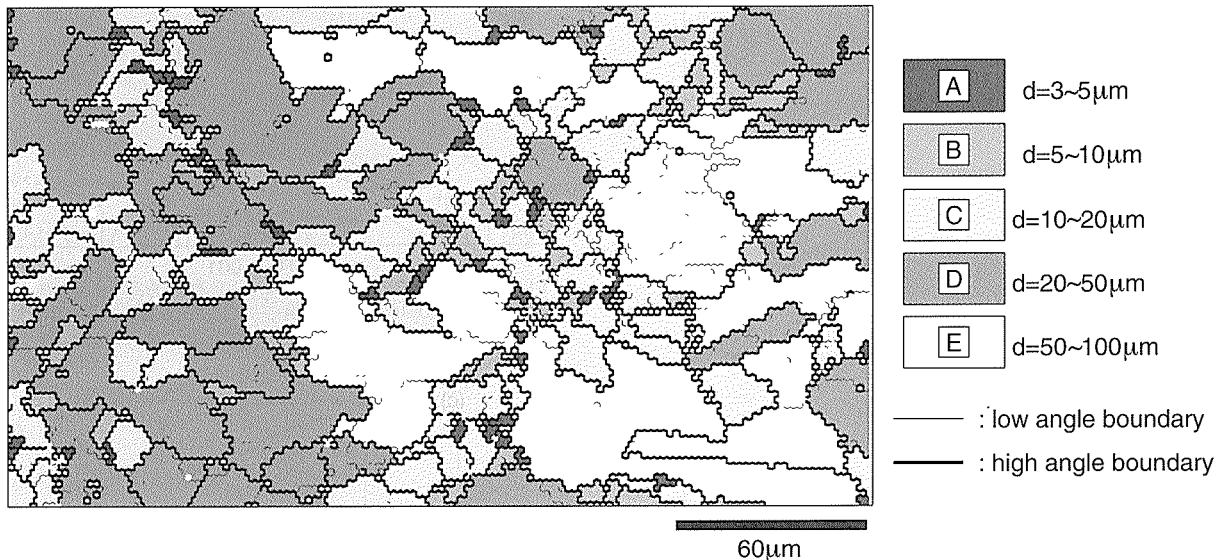


Fig. 10 Grain structure micrograph, constructed by EBSP, of a dynamically recrystallized area in the specimen deformed at high temperature ($T = 905\text{ K}$, $\dot{\epsilon} = 1.0 \times 10^{-4}\text{ s}^{-1}$, $\epsilon = -1.7$).

conditions of high temperatures and low strain rates where twinning occurs frequently during grain boundary migration⁶⁾ and hence new grains are formed with random orientation,¹¹⁾ a fraction of the length of twin boundaries to that of grain boundaries was only about 20% at most in the present deformation conditions. This suggests that the formation of weak texture cannot be attributed to twinning. Texture weakening should be understood in terms of the process of nucleation of grains. Since crystal orientations of new grains is considered to exist in the deformed state, the above fact that the texture is not so sharp indicates that, lattice rotation occurs locally in various directions in the vicinity of grain boundaries even in the same grain. The present authors consider that the undulation (to become wavy) of grain boundary is the precondition for the occurrence of severe, local lattice rotation.¹²⁾

A model for new grain formation, in which attention was paid to the undulation of grain boundary, was proposed by Miura *et al.*⁴⁾ and Belyakov *et al.*⁵⁾ According to the model, when wavy grain boundary slides, local lattice rotation occurs in a region where the boundary protrudes, and new grains are formed there. Although grain boundary sliding is expected to occur more easily at higher temperatures and lower strain rates, the orientation of new grains was not at random at these deformation conditions if twinning does not occur as in γ -TiAl.^{6,13,14)} Therefore, we would like to assert that, other than its sliding, the undulation of grain boundary itself has an effect on the generation of large, local lattice rotation and the resultant formation of new grains.

Optical microscopy and SEM revealed no evidence of void formation in grain boundaries, indicating that the continuity must be preserved in grain boundaries during deformation. Figure 12(a) is a schematic drawing of wavy grain boundary at the initial stage of DRX. Figures 12(b) and (c) are enlarged drawings of regions I and II in Fig. 12(a), respectively. When grain boundary exists on the xy plane (region I, Fig. 12(b)), the conditions on the strain component for preserving the con-

tinuity of deformation are given by^{15,16)}

$$\epsilon_{xx}^A = \epsilon_{xx}^B, \epsilon_{yy}^A = \epsilon_{yy}^B \text{ and } \gamma_{xy}^A = \gamma_{xy}^B.$$

In the neighboring part of the grain boundary (region II), however, the boundary does not exist on the xy plane (Fig. 12(c)). In this case, the constraint conditions for preserving the continuity of deformation in the grain boundary cannot be described by the above three equations. The undulation of grain boundary may complicate operative slip systems near grain boundary. That is, even in an identical grain, the kind, number and activity of operative slip systems may differ largely from place to place in the vicinity of wavy grain boundary. Such a local change in the slip activity may generate a large difference in the local lattice rotation, resulting in small regions with various crystal orientations that may act as nuclei of new grains.

As mentioned in Section 3.4.1, the misorientation was larger in the vicinity of grain boundary than in the grain center (Fig. 8). Further, the misorientation measured along grain boundary was larger for wavy boundaries after high temperature deformation than for smooth ones after room temperature deformation (compare Fig. 6 with Fig. 5), and it tended to be larger for a part of grain boundary where the degree of its curvature is larger (Fig. 7). Moreover, the orientation of lattice rotation axis was distributed at random (Fig. 6). These experimental facts support the above consideration for the generation of local lattice rotation and the formation of new grains in DRX.

4.3 Process of texture formation

Luton and Sellars¹⁷⁾ explained the shape of stress-strain curve during DRX on a basis of both the strain required for the onset of DRX ϵ_c and the strain from the onset to the end of DRX ϵ_x ; if ϵ_c is larger or smaller than ϵ_x , then the stress-strain curve becomes single-peak type or multi-peak type, respectively. In their explanation, DRX was considered to occur repeatedly after deformation of every strain of ϵ_c . Since then, it has been prevailing for the process of DRX that newly

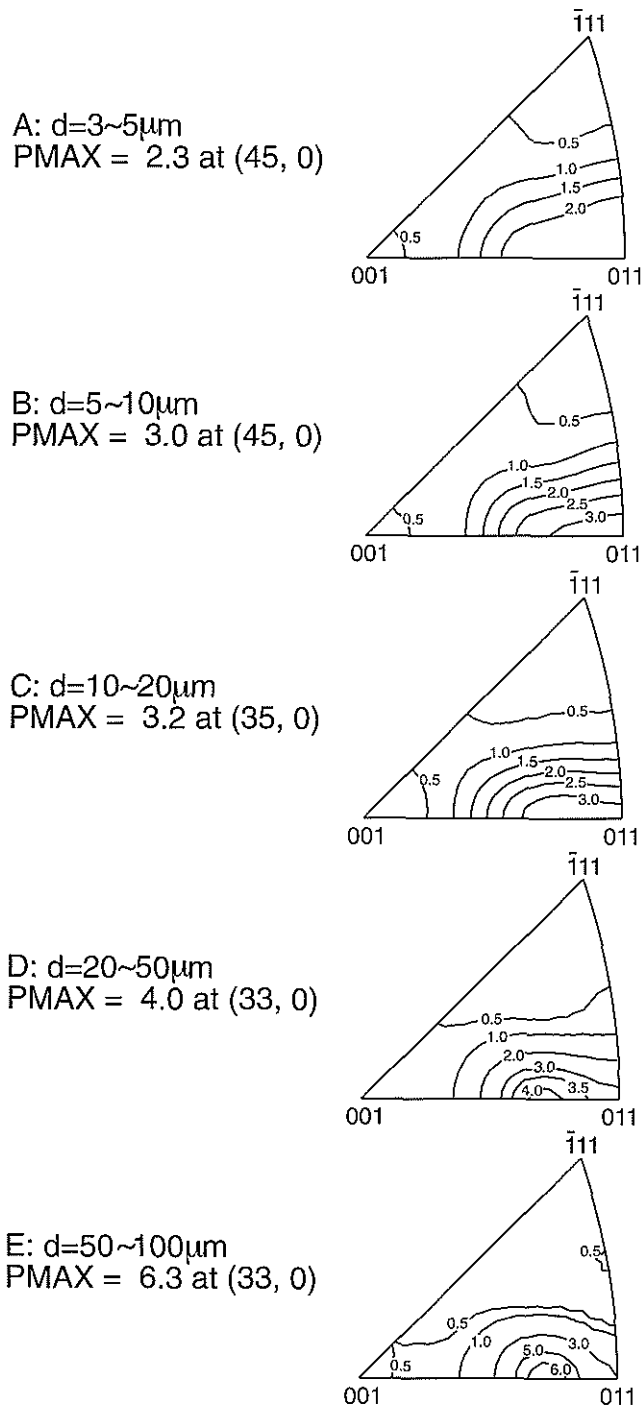


Fig. 11 Inverse pole figures of dynamically recrystallized grains with different grain sizes A to E in a fully recrystallized area in the specimen deformed at 905 K and a true strain rate of $1.0 \times 10^{-4} \text{ s}^{-1}$ up to a true strain of -1.7 .

formed grains deform and grow at the same time, and when these grains grow up to a certain size new grains are formed again in these grains, and so on. According to this consideration, the grown up grains ought to have the orientation of (011) that is the stable orientation for compression.⁶⁾ However, this expectation contradicts the experimental result that the coarse grains formed during DRX are not in the orientation of (011) but in the orientation of 12 degrees away from (011) to (001) (Fig. 11, D and E).

Main experimental results on microstructure and texture

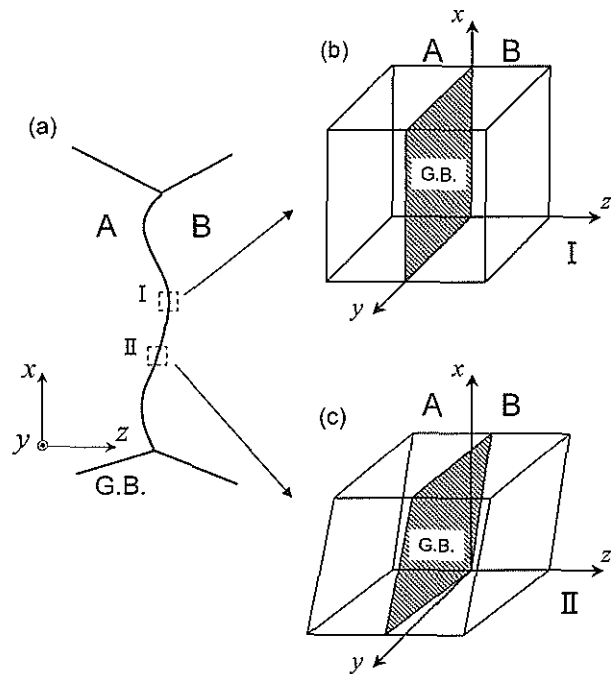


Fig. 12 Wavy grain boundary at the initial stage of dynamic recrystallization (a). Enlarged drawings of regions I and II are shown in (b) and (c), respectively. The orientation change of the grain boundary plane results in the change of activated slip systems along the boundary. Detailed description is given in the text.

obtained hitherto are summarized in the following three points.

- (1) New grains are formed in the vicinity of initial grain boundaries and their orientations are at random (sections 3.4.1 and 3.4.2).
- (2) The stable orientation for compression is (011).⁶⁾
- (3) Main component of texture formed during DRX is in the orientation of about 10 degrees away from (011) to (001).⁶⁾

The following process for DRX and texture formation are conclusively deduced from these results.

Newly formed grains grow up to a certain size, and then new grains with random orientations are formed again in the vicinity of grain boundaries of grown up grains. This process occurs repeatedly during DRX. Thus, small grains tended to exist together forming a group (Fig. 10). Such regions consisting of small grains are considered to be ones that have been subjected to severe deformation and will be consumed by new grains in further DRX, since small grains are in the orientation of (011) (Fig. 11, A and B). Moreover, randomly oriented new grains receive compressive deformation and change their orientation toward the stable orientation for compression (011). However, further nucleation of new grains occurs in random orientation before they reach (011), and as a result grains with the orientation close to (011) disappears. This is the reason why the main component of texture formed during DRX is not in the orientation of (011), but in the orientation of about 10 degrees away from (011) to (001).

5. Conclusions

To make clear the process of dynamic recrystallization (DRX) and resultant texture formation, polycrystalline pure nickel was deformed in compression at temperatures of 873 K and 905 K and true strain rates of $1.0 \times 10^{-3} \text{ s}^{-1}$ and $1.0 \times 10^{-4} \text{ s}^{-1}$ where new grains are formed through the so-called nucleation and growth mechanism. Microstructure at each stage of DRX was examined by optical microscopy and SEM, and crystal orientation of each grain was measured by the EBSP technique. Main conclusions obtained are summarized as follows.

(1) Initial grain boundaries become wavy prior to the formation of new grains. This undulation (to become wavy) of grain boundaries influences the orientation distribution in the vicinity of grain boundaries; the misorientation between neighboring points separated by an interval of a few μm becomes larger with an increase in the degree of grain boundary curvature.

(2) New grains are formed in the vicinity of grain boundaries in random orientation. This indicates that the undulation of grain boundaries causes large, local lattice rotation in various directions in their vicinity, resulting in the formation of new grains with random orientation.

(3) DRX from fully DRXed structure occurs by the formation of new grains with random orientation in the vicinity of grain boundaries of grown up grains. The interior of grown up, coarse grains is sometimes divided into small grains by severe deformation at high temperatures. Such regions consisting of small grains are regions to be encroached by new grains during further DRX.

(4) Texture develops though it is not so sharp. Randomly oriented new grains change their orientation toward the stable orientation for compression (011). However, further nucleation of new grains with random orientation occurs before they reach (011), and the number of grains with the orientation close to (011) reduces. This is the reason why the main

component of texture is in the orientation of about 10 degrees away from (011) to (001).

Acknowledgments

The authors would like to express their thanks to Dr. S. Takagi of Industrial Research Institute of Kanagawa for his help in using the machine of uniaxial compression tests. This work was financially supported by JSPS research for the future program. The authors greatly appreciate to the program.

REFERENCES

- 1) T. Sakai and J. J. Jonas: *Acta Metall.* **32** (1984) 189–209.
- 2) F. J. Humphreys and M. Hatherly: *Recrystallization and Related Annealing Phenomena*, (Pergamon, Oxford, 1995) pp. 373–374.
- 3) T. Maki and I. Tamura: *Tetsu-to-Hagane* **70** (1984) 2073–2080.
- 4) H. Miura, H. Aoyama and T. Sakai: *J. Japan Inst. Metals* **58** (1994) 267–275.
- 5) A. Belyakov, H. Miura and T. Sakai: *Mater. Sci. Eng. A255* (1998) 139–147.
- 6) H. Fukutomi, M. Hasegawa and M. Yamamoto: *J. Japan Inst. Metals* **65** (2001) 71–77.
- 7) T. Hasegawa, K. Kawaguchi, T. Murata and T. Yakou: *Mater. Trans., JIM* **32** (1991) 244–250.
- 8) Here, a very large of value θ (for example, 36.30° in the case of $0.4 \leq h/w$) was not taken into account since it might possibly appear because of some unknown error in measurement and its fraction is very low, indeed.
- 9) N. Tsuji, H. Yagi, Y. Matsubara and Y. Saito: presented at J. J. Jonas Symp. on Thermomechanical Processing, Texture and Formability of Steel COM 2000.
- 10) K. Ito: *J. JILM* **31** (1981) 497–507.
- 11) G. Gottstein: *Acta. Metall.* **32** (1984) 1117–1138.
- 12) M. Hasegawa, M. Yamamoto and H. Fukutomi: *Collected Abstracts of the 1999 Autumn Meeting of the Japan Inst. Metals* (1999) 549.
- 13) H. Fukutomi and M. Hasegawa: *Proc. of the 2001 Asian Symposium on Advanced Engineering and Science*.
- 14) M. Hasegawa and H. Fukutomi: unpublished work.
- 15) W. F. Hosford: *The Mechanics of Crystals and Textured Polycrystals*, (Oxford University Press, Oxford, 1993) pp. 112–113.
- 16) J. D. Livingston and B. Chalmers: *Acta Metall.* **5** (1957) 322–327.
- 17) M. J. Luton and C. M. Sellars: *Acta Metall.* **17** (1969) 1033–1043.